

Polymer Communication

High thermal conductivity of polyethylene nanowire arrays fabricated by an improved nanoporous template wetting technique

Bing-Yang Cao^{a,*}, Yuan-Wei Li^a, Jie Kong^{b,**}, Heng Chen^b, Yan Xu^c, Kai-Leung Yung^{c,***}, An Cai^d

^aKey Laboratory for Thermal Science and Power Engineering of Ministry of Education, Department of Engineering Mechanics, Tsinghua University, Beijing 100084, PR China

^bDepartment of Applied Chemistry, School of Science, Northwestern Polytechnical University, Xi'an 710072, PR China

^cDepartment of Industrial and Systems Engineering, The Hong Kong Polytechnic University, Hung Hom, Kowloon, Hong Kong, PR China

^dShanghai Institute of Ceramics, Chinese Academy of Sciences, Shanghai 200050, PR China

ARTICLE INFO

Article history:

Received 31 July 2010

Received in revised form

25 January 2011

Accepted 16 February 2011

Available online 23 February 2011

Keywords:

Polymer nanowire array

Thermal conductivity

Nanoporous template wetting

ABSTRACT

Generally polymer bulk structures and nanostructures are thermally insulative. In this study, we show that an improved nanoporous template wetting technique can prepare thermally conductive polymer nanowire arrays. The thermal conductivities of the fabricated high-density polyethylene (HDPE) nanowire arrays with diameters of 100 nm and 200 nm, measured by a laser flash method, are about 2 orders of magnitude higher than their bulk counterparts. The estimated thermal conductivity of a single HDPE nanowire is as high as 26.5 W/mK at room temperature. The high orientation of chains of the HDPE nanowires may arise from the integrative effects of shear rate, vibrational perturbation, translocation, nanoconfinement and crystallization. Findings in this study provide useful strategies on enhancing the intrinsic thermal properties of polymer nanostructures.

© 2011 Elsevier Ltd. All rights reserved.

1. Introduction

Arrays of polymer nanostructures have drawn much attention for their potential applications in the fields of electronics, mechanical, biomedical and fluidic nanodevices due to their unique properties in recent years [1–3]. Polymer nanostructure layers were also tried to control solid–solid interfacial thermal conductance [4–6]. However, that polymers generally have very low thermal conductivity of 0.1–1 W/mK and the thermal conductivities of nanostructures are further limited by boundary phonon scattering does not match the requirement for the ultrahigh density heat dissipation in most nanodevices yet [7]. Filling polymers with additives with high thermal conductivity, such as metallic nanoparticles or carbon nanotubes, or constructing heat transport networks are typical ways to increase their thermal transport [8,9]. The enhancement of the thermal conductivity of such nanocomposites, however, remains much lower than theoretical expectations because of the high thermal contact resistance at polymer–additive interfaces [10,11] and the decrease of the

additives' thermal conductivity affected by surroundings [12,13]. Therefore, increasing the intrinsic thermal conductivity of polymer nanostructures is highly desired.

Actually researchers have realized that polymers will exhibit significant anisotropy in thermal conductivity when the polymer chains are partially oriented [14]. Molecular dynamics simulations showed that a single chain or aligned chains might have extremely high thermal conductivity, ~350 W/mK or even divergent with chain length [15], since the heat transports along individual polymer chains in a ballistic way [16,17]. It has also been experimentally confirmed recently [18]. Normally, the random orientation of polymer chains with very weak couplings between them in amorphous polymers or amorphous phase semi-crystalline polymers shortens the mean free path of phonons, and results in the low thermal conductivity. If the polymer chains are aligned in a certain direction by spinning [19] or draw [20–22], the ballistic transport of heat will be increased and thus the thermal conductivity along this direction is greatly enhanced [23]. Drawn or spun polymer bulk structures were found to be able to give thermal conductivities of up to 50 W/mK [19–22].

Until most recently, Shen et al. applied this idea to fabricate gel-spun and ultra-drawn polyethylene (PE) nanofibers with very high thermal conductivity, ~104 W/mK [24]. This was attributed to the restructuring of the polymer chains by stretching that improved the nanofiber quality from a random orientation toward an ideal single crystalline fiber. It should be mentioned that there is still great

* Corresponding author. Tel./fax: +86 10 6278 1610.

** Corresponding author. Tel./fax: +86 29 8843 1688.

*** Corresponding author. Tel./fax: +852 2362 5267.

E-mail addresses: caoby@tsinghua.edu.cn (B.-Y. Cao), kongjie@nwpu.edu.cn (J. Kong), mfklyung@inet.polyu.edu.hk (K.-L. Yung).

challenge in uniform and massive production for ultra-drawn nanowires. Due to phonon scattering and less orientation, the reported thermal conductivities of polymer nanofilms were still very low [4–6]. Thus far, there is seldom report on thermal conductivity of polymer nanowire arrays.

In this paper we report on high thermal conductivity of high-density polyethylene (HDPE) nanowire arrays. The HDPE nanowire arrays with diameters of 100 nm and 200 nm are fabricated by using an improved nanoporous template wetting technique. The thermal conductivity of the as-prepared nanowire arrays is measured by a laser flash method. We find that the arrays have high thermal conductivity of about 2 orders higher than that of HDPE bulk material. The underlying mechanisms for the high orientation of polymer chains are also demonstrated.

2. Fabrication of HDPE nanowire arrays

The nanoporous template wetting technique, originally developed by Steinhart et al. [25], is now improved to enhance the polymer infiltration into the nanopores by a high-frequency fluid pulsation strategy as shown in Fig. 1. The porous anodic alumina (PAA) templates with pore diameters of 100 nm and 200 nm are purchased from Whatman, Inc. The PAA templates are freestanding disks with a diameter of 13 mm, and their pores are all through-hole. The PAA templates are firstly treated with solvents of different polarities, i.e. ethanol, acetone, chloroform and hexane in sequence. The HDPE films with thickness of about 300 μm , density of 0.945 g/cm^3 and melting index of 13.0 $\text{g}/10 \text{ min}$ are obtained from Qilu Petroleum and Chemical Co. of China. An HDPE film is then placed on the top of a template with a good contact. The chamber containing the PE film and template sample is then heated to 160 $^\circ\text{C}$ by thermal cycle springs, well above the melting point of HDPE (130 $^\circ\text{C}$), to excite the infiltration of the PE melts into the nanopores of the template. During the infiltration process, a vibration with a frequency about $\sim 10 \text{ kHz}$ induced by a piezoelectric transducer is imposed. This technique is able to produce several times longer polymer nanowires compared with the original wetting template technique [26]. It indicates that the infiltration is dominated by vibrational hydrodynamics rather than just by wetting behaviors.

Moreover, the vibration does help the polymer chains to be more oriented due to the oscillatory shear rates [27]. This process generally takes about 1 h to produce HDPE nanowire arrays with about 50 μm thickness. After that, the sample is taken out of the hot chamber, and cooled down to ambient temperature. The cooling process often takes about 1 h. The HDPE nanowire arrays are then released by removing the template in NaOH aqueous solution and being rinsed with deionized water and ethanol and being dry at 30 $^\circ\text{C}$ in vacuum in sequence.

The cross-section and top view images, characterized by scanning electron microscopy (SEM, Leica Stereoscan 440) and field-emission scanning electron microscopy (FE-SEM, JEOL JSM-6335F), of the as-fabricated HDPE nanowire array are shown in Fig. 2 in which the nanowire array with diameter of 200 nm is taken as a case study. The nanowires are of high quality, such as well-defined, straight, smooth in surface and uniform in diameter, thanks to the good PAA templates. We also do the energy-dispersive X-ray spectroscopy analysis and find there is no residue alumina left in the film, which ensures that we can measure the intrinsic thermophysical property of the polymer nanowires. The whole sample for thermal conductivity measurements is consisted of two layers with inhomogeneous properties. One is the substrate layer that solidifies from the redundant HDPE melts outside of the templates. The other is the nanowire array layer. By measuring the SEM images, we can obtain the thicknesses of the overall sample L_0 , the substrate layer L_s , and the nanowire array layer L_{nw} ($L_0 = L_s + L_{nw}$). For the 100 nm diameter nanowire array $L_s = 163 \mu\text{m}$ and $L_{nw} = 50 \mu\text{m}$ ($L_0 = 213 \mu\text{m}$). For the 200 nm diameter nanowire array $L_s = 160 \mu\text{m}$ and $L_{nw} = 60.6 \mu\text{m}$ ($L_0 = 220.6 \mu\text{m}$). One of the most important points is that there is no thermal contact resistance between the two layers, which enables the accurate extraction of thermal conductivity of the nanowire array from measuring the thermal conductivity of the whole sample.

3. Measurement setup and analytical method

A laser flash technique, schematically shown in Fig. 3, is employed to measure the thermal conductivity of the HDPE nanowire arrays. The technique has advantages of no thermal

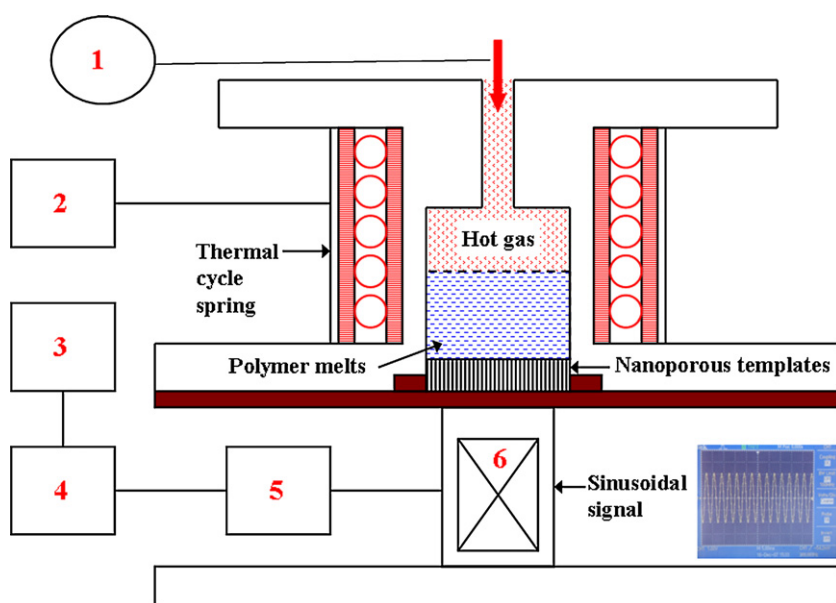


Fig. 1. Schematic of the fabrication system by the improved nanoporous template wetting technique with high-frequency vibrational perturbation. In the figure: (1) pressure meter, (2) temperature controller (KTM4, Panasonic, Japan), (3) oscilloscope (TDS2014, Tektronix), (4) alternating current generator (MSO6054A, Agilent Technologies), (5) piezoelectric amplifier (HVPVT, Physik Instrument, Germany), (6) piezoelectric transducer (P-244.1X, Physik Instrument, Germany).

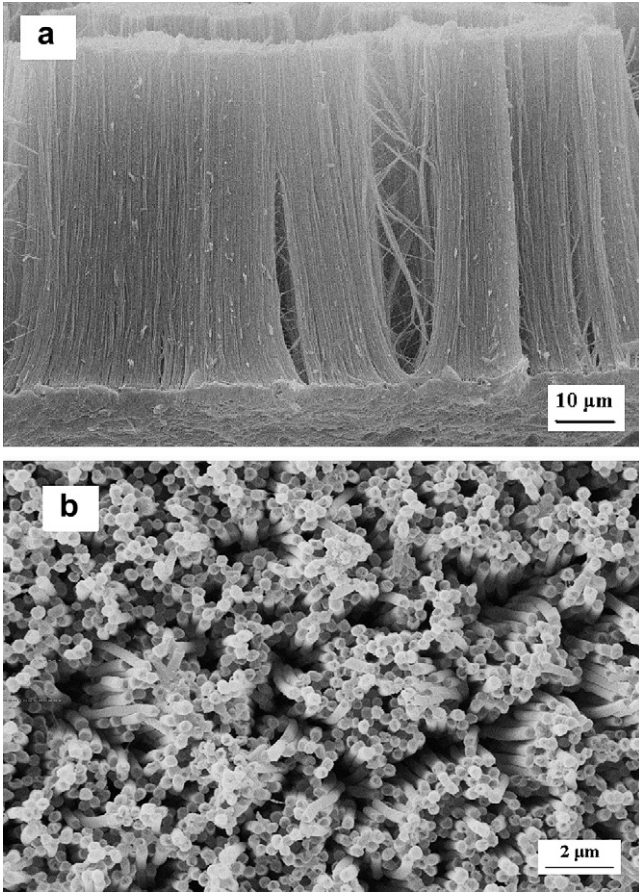


Fig. 2. Cross-section (a) and top view (b) SEM images of the HDPE nanowire array. The nanowire array with 200 nm in diameter is taken as a case study.

contact resistance and very small heat losses, and has been applied to measure the thermal properties of polymer [21,22], metallic [28], carbon nanotube [29], and nanocomposite [30] films. The samples are placed in a vacuum chamber with a pressure of about 0.1 Pa to reduce the heat losses. A nanosecond laser pulse with a pulse width of 6 ns and a wavelength of 1064 nm from a Q-switched Nd:YAG laser (Continuum Surelite I-10) is used to irradiate the substrate layer's surface. The surface is opaque by depositing ~2 μm thick Au and ~2 μm thick graphite in sequence. The temperature rise of the rear surface, i.e. the nanowire array's surface, will give a corresponding infrared emission variation, which is detected by a liquid-

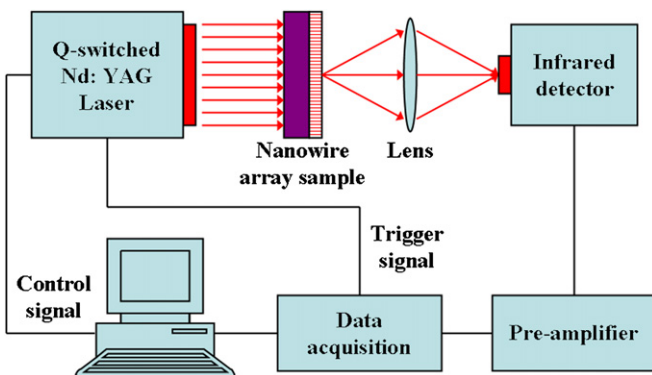


Fig. 3. Schematic diagram of the experimental system by a laser flash technique.

nitrogen-cooled photovoltaic type of mercury cadmium telluride detector. Theoretically, the temperature rise follows [28]

$$T(t) = \frac{Q}{\rho_0 c_{p0} L_0} \left[1 + 2 \sum_1^{\infty} (-1)^n \exp\left(\frac{-n^2 \pi^2}{L_0^2} \alpha_0 t\right) \right], \quad (1)$$

where Q is the absorbed energy per unit area, α_0 is the overall thermal diffusivity, ρ_0 is the overall density, c_{p0} is the overall specific heat, and L_0 is the overall thickness, keeping in mind that the double-layer sample is inhomogeneous in thermal properties. Divided by the maximum temperature rise $T_{\max} = Q/(\rho_0 c_{p0} L_0)$, the rescaled temperature rise is only related to the thermal diffusivity and thickness

$$\theta(t) = 1 + 2 \sum_1^{\infty} (-1)^n \exp\left(\frac{-n^2 \pi^2}{L_0^2} \alpha_0 t\right). \quad (2)$$

By detecting the normalized temperature rise, we can obtain the overall thermal diffusivity of the whole sample, and then the thermal conductivity of the nanowire array can be extracted.

The measured normalized temperature rise is typically shown in Fig. 4, which is indicative of agreement with the theoretical prediction of Eq. (2). For double-layer films, the overall apparent thermal conductivity, which regularly depends on individual thermal conductivities of the two layers, is able to be accurately measured by the laser flash method with the overall parameters properly defined [31]. Following the rule in Ref. 31, the overall density and specific heat of the whole sample are, respectively, defined as:

$$\rho_0 = \frac{\rho[L_s + L_{nw}\phi]}{L_0}, \quad (3a)$$

$$c_{p0} = \frac{c_p[L_s + L_{nw}\phi]}{L_0}. \quad (3b)$$

where $\rho = 945 \text{ kg/m}^3$ is the density of HDPE, $c_p = 1900 \text{ J/kgK}$ is the specific heat of HDPE, L_s is the thickness of the substrate layer, L_{nw} is the thickness of the nanowire array layer, and ϕ is the porosity, ratio of the pore-to-total volumes, of the PAA templates. We assume that the density and specific heat of the nanofibers are the same as those of the substrate since both the parameters are not sensitive to the crystallinity at room temperature [32,33] (we show below that the nanofibers are in high orientation). The porosities of the templates

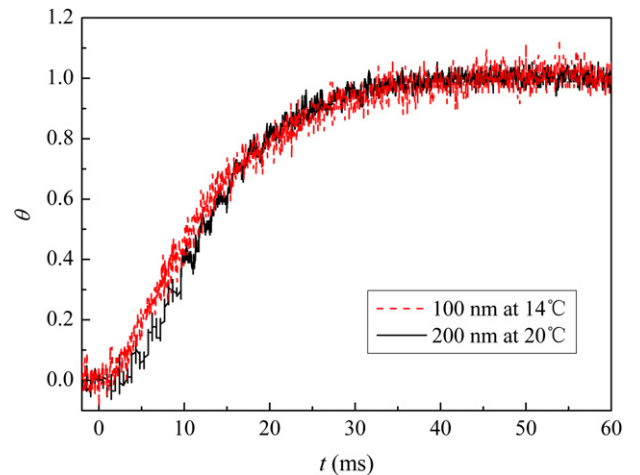


Fig. 4. Typical measured normalized temperature rise of the nanowire array's surface varying along with time.

with pore diameters of 100 nm and 200 nm are 0.572 and 0.424, respectively. Ideally the overall thermal diffusivity of the whole sample can be extracted by

$$\alpha_0 = \frac{0.138L_0^2}{t_{1/2}}, \quad (4)$$

where $t_{1/2}$ is the time for the temperature rises to 1/2 of the maximum value. However, the thermal conductivity will be over-estimated if heat losses exist. For handling unexpected heat losses, we use Degiovanni's expression to calculate the overall thermal diffusivity [34]

$$\alpha_0 = \frac{L_0^2}{t_{5/6}} \left[0.8498 - 1.8451 \frac{t_{1/3}}{t_{5/6}} + 1.0315 \left(\frac{t_{1/3}}{t_{5/6}} \right)^2 \right], \quad (5)$$

where $t_{1/3}$ and $t_{5/6}$ refer to times for the temperature rises to 1/3 and 5/6 of the maximum value, respectively. The overall thermal conductivity is given by $\lambda_0 = \alpha_0 \rho_0 c_{p0}$. The overall thermal resistance of the whole double-layer sample, $R_0 = L_0/\lambda_0$, is consisted of the thermal resistances of the substrate layer, $R_s = L_s/\lambda_s$, and nanowire array layer, $R_{nw} = L_{nw}/\lambda_{nw}$. We can obtain

$$\frac{L_0}{\lambda_0} = \frac{L_s}{\lambda_s} + \frac{L_{nw}}{\lambda_{nw}}. \quad (6)$$

Then, the thermal conductivity of the nanowire array can be extracted by;

$$\lambda_{nw} = \frac{L_{nw}\lambda_s\lambda_0}{L_0\lambda_s - L_s\lambda_0}. \quad (7)$$

The thermal conductivity of the substrate layer, λ_s , is obtained by measuring an HDPE film with thickness of about 300 μm . λ_s is about 0.5 W/mK and is not sensitive to temperature considering the present temperature range 10–80 °C. The total experimental error in thermal diffusivity is estimated within 5%.

4. Results and discussion

The measured overall thermal diffusivity and thermal conductivity of the whole samples are shown in Fig. 5. We can see that the overall thermal conductivity of the nanowire array samples has been greatly enhanced by the nanofibers compared with the bulk HDPE thermal conductivity, ~ 0.5 W/mK. The sample with 100 nm diameter nanofibers has a higher overall thermal conductivity than

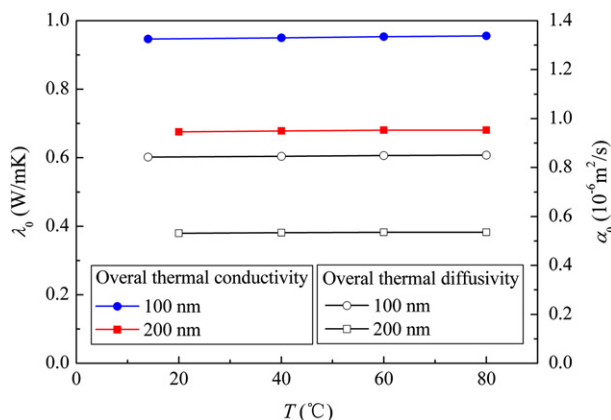


Fig. 5. The measured overall thermal diffusivity and thermal conductivity of the whole HDPE nanowire array samples.

that with 200 nm diameter nanofibers. The thermal diffusivity of the bulk HDPE is about $0.28 \times 10^{-6} \text{ m}^2/\text{s}$. Fig. 5 shows that the overall thermal diffusivity of the nanowire array samples is much larger than the bulk value because the overall thermal conductivity of the samples is enhanced but the overall density and specific heat are both decreased by the nanowire arrays.

The extracted thermal conductivities of the fabricated HDPE nanowire arrays are in the order of 10 W/mK as shown in Fig. 6. The thermal conductivity of the 100 nm diameter HDPE array at room temperature is 14.8 W/mK, about 30 times that of the bulk counterpart (~ 0.5 W/mK). The 200 nm diameter nanowire array has a thermal conductivity of 8.7 W/mK. The well-aligned spuncast polymer films were reported to have an effective thermal conductivity of only 0.20 W/mK [6]. The commercial thermally conductive silicon grease only has a thermal conductivity of ~ 2 W/mK. The present fabrication of nanowire arrays seems very promising for controlling interfacial thermal conductance. With the temperature increasing from room temperature to 80 °C, the thermal conductivity of the nanowire array with diameter of 200 nm increases to 13.8 W/mK, and the value of the array with 100 nm diameter increases to 21.1 W/mK. That the thermal conductivity increases slightly with the increasing temperature agrees well with previous observations [20–22], and is indicative of nearly constant mean free path of phonons. It should be noted that the thermal conductivity of the 100 nm diameter nanowire array is sort of higher than that of the 200 nm diameter array, which implies that the polymer chains of the as-prepared nanowires with smaller diameter may be more oriented. This tendency is opposite to the traditional size effects caused by boundary phonon scattering [7] but is in agreement with thermal transport in low-dimensional nanostructures, e.g. carbon nanotubes [35,36], which is indicative of the domination of the ballistic thermal transport instead of the diffusive way.

The thermal conductivities of individual nanowires are also estimated from dividing the measured values by the template porosities with ignoring inevitable phonon scattering between the nanowires, also as shown in Fig. 6. This means that it gives only the lowest bound predictions of thermal conductivities. At room temperature, the estimated thermal conductivities are 26.5 W/mK and 20.5 W/mK for individual nanowires with 100 nm and 200 nm diameters, respectively. At 80 °C, the estimated values reach 36.5 W/mK and 32.6 W/mK, which are nearly 2 orders of magnitude higher than that of HDPE bulk structure. Compared with the ultra-drawn PE nanowires by Shen et al. [24], the orientation of

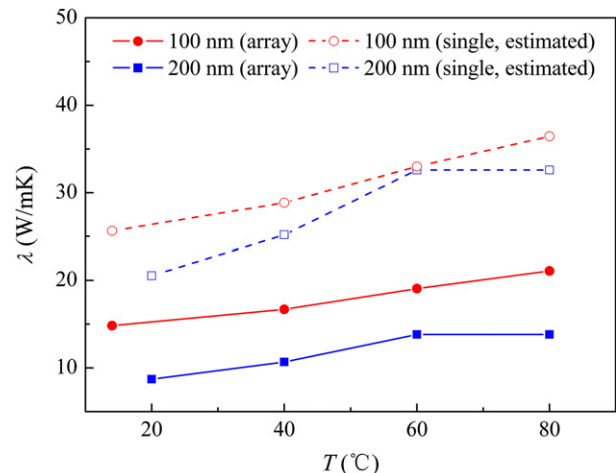


Fig. 6. The extracted thermal conductivity of HDPE nanowire arrays and the estimated thermal conductivity of individual nanowires.

chains of the present polymer nanowires is estimated to be equivalent to draw ratios of about 50–100. The thermal conductivities of the present HDPE nanowires are not as high as those of ultra-drawn PE nanowires reported in Ref. 24. The reason is because the polymer chains are less aligned and we do not take into account the effects of boundary phonon scattering. Despite this, we believe that there is still room for the enhancement of the intrinsic thermal conductivity of the polymer nanowire arrays regarding further improvement of the fabrication. What's more, these nanowire arrays should be promising for engineering applications due to the simple but massive, high-quality and low-cost production.

The present thermal conductivity enhancement of polymer nanowires is quite different from the traditional size effects that the thermal property of a nanostructure material is often lowered due to the boundary scattering of phonons [7,37–39]. This enhancement may be attributed to the high chain orientation of the HDPE nanowire arrays. Several factors should be possibly taken into account. First, when infiltrating polymer melts into template nanopores, the polymer melts is subjected to shear rates so that the chains become more oriented and the thermal conduction along the shear direction will be enhanced [40,41]. It was reported that an oscillatory shear, as induced by the piezoelectric transducer in the present fabrication process, could help to order polymer chains [27]. Second, long polymer chains may be well aligned when translocating through small nanopores, which is just the case in the present fabrication process, as reviewed in Ref. [42]. Third, when preparing nanowire arrays by wetting nanoporous alumina template with polymer melts, the nanoconfinement, i.e. the interaction between polymer chains and the alumina pore's walls with high surface energy, may also improve the polymer crystal orientation along the axis greatly. This confinement effect was experimentally observed by Garcia-Gutierrez et al. [43], and Mhanandia et al. [44], most recently. The orientation of polymer melts is rationally expected to be remained during the solidification since the relaxation time of nanoconfined matters can be prolonged by several orders of the bulk value [45]. Fourth, the crystallinity of polymer nanofibers, which may dominate the final orientation of polymer nanofibers, was reported to depend on many factors, such as pore size and cooling rate [46]. Further studies toward this issue should be carried out in the future. Hopefully, the integrative effects by shear rate, vibrational perturbation, translocation, nanoconfinement and crystallization should play important roles in the high orientation of the PE nanowires fabricated by the improved vibrational nanoporous template wetting technique though we are not sure whether other unpredictable factors exist.

5. Conclusion

We have fabricated thermally conductive HDPE nanowire arrays with diameters of 100 nm and 200 nm by an improved vibrational nanoporous template wetting technique. The thermal conductivities of the as-prepared nanowire arrays are measured by a laser flash method. It is found that the thermal conductivities are in the order of 10 W/mK, nearly 2 orders of magnitude higher than their bulk structure. The estimated thermal conductivity of individual HDPE nanowires can reach 26.5 W/mK at room temperature, which indicates that the nanowires have an equivalent orientation to ultra-drawn nanofibers with draw ratios of 50–100. In particular, we find that the as-prepared nanowires with smaller diameters have higher thermal conductivities, which is indicative of the domination of the ballistic thermal transport. The integrative effects of shear rate, vibrational perturbation, translocation, nanoconfinement and crystallization may be responsible for the high orientation of the HDPE nanowires. The as-fabricated nanowire arrays with high thermal conductivity, as well as advantages in

simple but massive, high-quality and low-cost production, will supply a promising platform for micro/nanoscale devices.

Acknowledgment

We are very grateful to the reviewers for their in-depth suggestions towards improving our manuscript. This work is financially supported by the National Natural Science Foundation of China (No. 50976052, 50730006, 50706057) and Aero-Science Fund of China (No. 2009ZH53073), Chunhui Plan of Ministry of Education of China (Z2009-1-71004), Aoxiang Star Project in Northwestern Polytechnical University, and funding from the Hong Kong Research Grants Council (Polyll 5347/08E).

References

- [1] Tang C, Lennon EM, Fredrickson GH, Kramer EJ, Hawker CJ. *Science* 2008;32:1679–84.
- [2] Hu ZJ, Tian MW, Nysten B, Jonas AM. *Nat Mater* 2009;8:62–7.
- [3] Ryan AJ. *Nature* 2010;456:334–6.
- [4] Wang RY, Segalman RA, Majumdar A. *Appl Phys Lett* 2006;89:173113.
- [5] Jin JZ, Manoharan MP, Wang Q, Haque MA. *Appl Phys Lett* 2009;95:033113.
- [6] Losego MD, Moh L, Arpin KA, Cahill DG, Braun PV. *Appl Phys Lett* 2010;97:011908.
- [7] Cahill DG, Ford WK, Goodson KE, Mahan GD, Majumdar A, Maris HJ, et al. *J Appl Phys* 2003;93:793–818.
- [8] Varshney V, Patnaik SS, Roy AK, Farmer BL. *Polymer* 2009;50:3378–85.
- [9] Zhao L, Crombez R, Caballero FP, Antonietti M, Texter J, Titirici MM. *Polymer* 2010;51:4540–6.
- [10] Huxtable ST, Cahill DG, Shenogin S, Xue LP, Ozisik R, Barone P, et al. *Nat Mater* 2003;2:731–4.
- [11] Clancy TC, Gates TS. *Polymer* 2006;47:5990–6.
- [12] Padgett CW, Brenner CW. *Nano Lett* 2004;4:1051–3.
- [13] Cao BY, Hou QW. *Chin Phys Lett* 2008;25:1392–5.
- [14] Kurabayashi K. *Int J Thermophys* 2001;22:277–88.
- [15] Henry A, Chen G. *Phys Rev Lett* 2008;101:235502.
- [16] Henry A, Chen G. *Phys Rev B* 2009;79:144305.
- [17] Ni B, Watanabe T, Phillpot SR. *J Phys Condens Matter* 2009;21:084219.
- [18] Wang ZH, Carter JA, Lagutchev A, Koh YK, Seong NH, Cahill DG, et al. *Science* 2007;317:787–90.
- [19] Choy CL, Fei Y, Xi TG. *J Polym Sci B Polym Phys* 1993;31:365–70.
- [20] Choy CL, Luk WK, Chen FC. *Polymer* 1978;19:155–62.
- [21] Choy CL, Wong YW, Yang GW, Kanamoto T. *J Polym Sci B Polym Phys* 1999;37:3359–67.
- [22] Fujishiro H, Ikebe M, Kashima T, Yamanaka A. *Jpn J Appl Phys* 1998;37:1994–5.
- [23] Liu J, Yang RG. *Phys Rev B* 2010;81:174122.
- [24] Shen S, Henry A, Tong J, Zheng RT, Chen G. *Nat Nanotech* 2010;5:251–5.
- [25] Steinhart M, Wendorff JH, Greiner A, Wehrspohn RB, Nielsch K, Schilling J, et al. *Science* 2002;296:1997.
- [26] Kong J, Xu Y, Yung KL, Xie YC, He L. *J Phys Chem C* 2009;113:624–9.
- [27] Rendon S, Burghardt WR, Auad ML, Kornfield JA. *Macromolecules* 2007;40:6624–30.
- [28] Ohta H, Shibata H, Waseda Y. *Rev Sci Instrum* 1989;60:317–21.
- [29] Abdalla M, Cai A, Wang XW. *Phys Lett A* 2007;369:120–3.
- [30] Abdalla M, Dean D, Theodore M, Fielding J, Nyairo E, Price G. *Polymer* 2010;51:1614–20.
- [31] Absi J, Smith DS, Nait-Ali B, Grandjean S, Berjonnaux J. *J Euro Ceram Soc* 2005;25:367–73.
- [32] Wunderlich B. *J Chem Phys* 1962;37:1203–7.
- [33] Wunderlich B. *Thermal analysis of polymeric materials*. Berlin, Heidelberg: Springer-Verlag; 2005.
- [34] Degiovanni A. *Rev Gen Therm (France)* 1977;185:420–41.
- [35] Dhar A. *Adv Phys* 2008;57:457–537.
- [36] Fujii M, Zhang X, Xie HQ, Ago H, Takahashi K, Ikuta T, et al. *Phys Rev Lett* 2005;95:065502.
- [37] Chen G. *Int J Thermal Sci* 2000;39:471–80.
- [38] Liang XG. *Chin Sci Bull* 2007;52:2457–72.
- [39] Cao BY, Li YW. *J Chem Phys* 2010;133:024106.
- [40] Venerus DC, Schieber JD, Balasubramanian V, Bush K, Smoukov S. *Phys Rev Lett* 2004;93:098301.
- [41] Yung KL, He L, Xu Y, Kong J. *Polymer* 2008;49:2770–4.
- [42] Meller A. *J Phys Condens Matter* 2003;15:R581–607.
- [43] Garcia-Gutierrez MC, Linares A, Hernandez JJ, Rueda JJ, Ezquerro TA, Poza P, et al. *Nano Lett* 2010;10:1472–6.
- [44] Mhanandia P, Schneider JJ, Khanef M, Stuhn B, Peixoto TP, Drossel B. *Phys Chem Chem Phys* 2010;12:4407–17.
- [45] Granick S. *Science* 1991;253:1374–9.
- [46] Martin J, Mijangos C, Sanz A, Ezquerro TA, Nogales A. *Macromolecules* 2009;42:5395–401.